Progress In Electromagnetics Research C, Vol. 106, 199–213, 2020

Analysis and Design of an Efficient Distance Less-Sensitive Wireless Power Transfer System

Meng Wang, Li Ren, Weina Liu, Yanyan Shi*, and Youtian Niu

Abstract—A traditional magnetic resonant coupling wireless power transfer (MRC-WPT) system is highly sensitive to the distance between transmitting and receiving coils. The transfer performance deteriorates at short distance due to magnetic over-coupling and magnetic weak-coupling at long distance which also results in the decrease of power. In order to improve the power transfer ability, this paper presents an MRC-WPT system with a novel design of resonant loops. Unlike the conventional system in which the receiving coil is identical with the transmitting coil, the receiving coil in the proposed system is different from the transmitting coil in terms of distance between turns. Theoretical equivalent models are presented to investigate the impact of the mutual inductance on the transfer efficiency. Based on numerical simulation, it is found that relatively more uniform mutual inductance can be obtained with the proposed resonant loops. With the proposed MRC-WPT system the results show that the power transfer ability at short and long distances is improved. The average transfer efficiency is enhanced about 10% compared with the conventional system. Furthermore, the sensitivity of the proposed MRC-WPT system to lateral and angular misalignments is studied and compared with the conventional system. An experimental prototype of the proposed MRC-WPT system is designed for validation. The results show that the performance of the proposed MRC-WPT system outperforms the conventional system without adding any complicated control circuits.

1. INTRODUCTION

In the past few years, wireless power transfer (WPT) has attracted a great deal of research interest [1]. With this technique, the power can be delivered wirelessly which avoids the traditional wire connection. Due to its advantages of safety, mobility, convenience, and reliability, WPT has been applied in a variety of applications such as contactless charging of electric vehicles [2, 3], medical implanted devices [4, 5], and consumer electronics [6, 7]. Typically, WPT can be categorized into two different types which are magnetic inductive coupling WPT (MIC-WPT) and magnetic resonant coupling WPT (MRC-WPT) [8, 9]. Among them, MIC-WPT is gradually becoming mature, and a large number of studies have been carried out [10–12]. The transfer efficiency can be up to over 90%, and the transfer power is from a few microwatts to several hundred kilowatts. However, MIC-WPT is weakly coupled, and the transfer distance is about several millimeters even if the transmitting and receiving loops are optimized to operate at a specific frequency. In addition, coil misalignment severely causes the drop of power delivered to loads. In comparison, strongly coupled MRC-WPT has gained increasing interests ever since it was introduced in 2007 [13]. It has been demonstrated that the power can be transferred in a longer distance if the transmitter and receiver are designed to resonate at the same frequency. Besides, MRC-WPT is less sensitive to misalignment between loops. As a result, MRC-WPT has received much attention due to its practical midrange transfer [14–16]. However, a common problem found in the MRC-WPT is the fact that frequency splitting occurs in the over-coupled region [17–21]. The

Received 11 September 2020, Accepted 26 October 2020, Scheduled 31 October 2020
* Corresponding author: Yanyan Shi (yyshi113@hotmail.com).
The authors are with the College of Electronic and Electrical Engineering, Henan Normal University, Xinxiang, Henan 453007, China.

transfer efficiency suffers from dramatic decrease. In the previous research, it has been revealed that the frequency at which the transfer efficiency peaks deviates from the tuned resonant frequency when the transfer distance decreases below a certain value. Instead, transfer efficiency peaks at two different frequencies which are above and below the resonant frequency.

To suppress frequency splitting, maximum efficiency tracking control is the most common solution in which the drive frequency is regulated to maximize the transfer efficiency in the over-coupled region [22, 23]. Nevertheless, the MRC-WPT system is relatively complicated with additional frequency tuning circuits, and the frequency is required to be adjusted at each transfer distance in real time. Impedance matching is another alternative to address the frequency splitting phenomenon for fixed-frequency MRC-WPT [24, 25]. At each transfer distance, an impedance matching network is needed to switch impedance to a corresponding matching channel for high transfer efficiency which complicates the system. To inhibit frequency splitting, switchable configurations provide another solution [26–28], which also make the system complicated as extra tuning circuits are required. Additionally, changing the configuration or regulating the angle of resonant loops is also proposed to suppress the frequency splitting without extra complex circuits. It is based on the consideration that frequency splitting is generated by magnetic over-coupling, and smoothing the rapid increase of mutual inductance is a feasible solution to improve transfer efficiency [29–31]. Aside from frequency splitting, the misalignment between transmitter and receiver also has an impact on the performance of the MRC-WPT [32–34].

This paper presents an MRC-WPT system with a novel configuration of resonant loops. In the conventional MRC-WPT system, two identical coils have been respectively adopted as the transmitting coil and receiving coil. Unlike this, the receiving coil designed in this work is different from the transmitting coil in terms of distance between turns while the total wire length is the same for the coils. Section 2 presents the analytical function of the transfer efficiency based on equivalent model of a typical MRC-WPT system. The impact of mutual inductance on the transfer efficiency is discussed, and frequency splitting is explained. To inhibit frequency splitting, a novel configuration for resonant loops is proposed. In Section 3, the effect of the distance between turns on the performance of MRC-WPT system is studied, and the optimal resonant loops are designed with distance less-sensitive characteristic. The performance of the proposed MRC-WPT system under lateral and angular misalignments is also investigated. In Section 4, a prototype of the proposed MRC-WPT system is developed. Experimental results are reported and compared with those obtained with the conventional MRC-WPT system. Finally, conclusions are drawn in Section 5.

2. THEORETICAL ANALYSIS

A typical MRC-WPT system consists of a power source, a transmitting loop, a receiving loop, and a load. In the MRC-WPT system, the resonant loops can be regarded as a two-port network, in which the transmitting coil is connected with the power source and the receiving coil connected with the load, respectively. With the assumption of a two-port network, the MRC-WPT system can be analyzed by scattering matrix parameters, as illustrated in Fig. 1.

In terms of S-parameters, the transfer efficiency of the MRC-WPT system η can be calculated as the ratio of the power dissipated at the load P_L to the power delivered to the input of the two-port

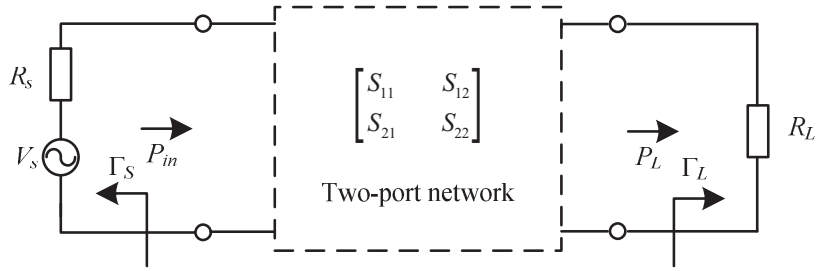

Figure 1. Equivalent model of the MRC-WPT system.

network P_{in} [35]

$$\eta = \frac{P_L}{P_{in}} = \frac{\left(1-|\Gamma_S|^2\right)\left(1-|\Gamma_L|^2\right)|S_{21}|^2}{\left|\left(1-S_{11}\Gamma_S\right)\left(1-S_{22}\Gamma_L\right)-S_{12}S_{21}\Gamma_S\Gamma_L\right|^2} \tag{1}$$

in which

$$\Gamma_S = \frac{R_S - R_0}{R_S + R_0}, \quad \Gamma_L = \frac{R_L - R_0}{R_L + R_0} \tag{2}$$

where S is the scattering parameter; Γ is the reflection coefficients; R_S and R_L are internal resistance of the source and the resistance of the load; and R_0 is the characteristic impedance of the transmission line with the most common industry standard being $50\,\Omega$ [36].

In this paper, the source and load impedance is assumed to match the characteristic impedance. Therefore, $\Gamma_S = \Gamma_L = 0$ and the transfer efficiency can be simplified to

$$\eta = |S_{21}|^2 = \left|\frac{2V_L}{V_S}\sqrt{\frac{R_S}{R_L}}\right|^2 \tag{3}$$

where V_S and V_L are respectively power source and load voltage.

Figure 2 shows the equivalent circuit of the MRC-WPT system. Resonant loops are modeled by the total resistance, self-inductance, and resonant capacitance which are connected in series. Based on Kirchhoff's voltage law, it can be obtained as:

$$\begin{pmatrix} V_S \\ 0 \end{pmatrix} = \begin{pmatrix} R_S + R_t + \mathrm{j}\omega L_t + \dfrac{1}{\mathrm{j}\omega C_t} & \mathrm{j}\omega M \\ \mathrm{j}\omega M & R_L + R_r + \mathrm{j}\omega L_r + \dfrac{1}{\mathrm{j}\omega C_r} \end{pmatrix} \begin{pmatrix} I_t \\ I_r \end{pmatrix} \tag{4}$$

where R_t and R_r represent the total resistance of the transmitting and receiving loops, respectively; L_t and L_r are the equivalent inductances of the loops; C_t and C_r are the resonant capacitances; M is the mutual inductance between resonant loops; I_t and I_r are the currents flowing in the loops; and ω is the driving angular frequency of the source.

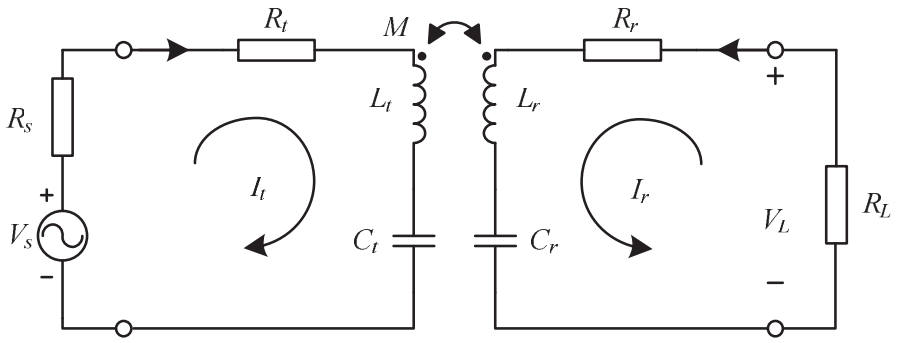

Figure 2. Equivalent circuit of the MRC-WPT system.

The load voltage can be given as:

$$V_L = -I_r R_L \tag{5}$$

Based on Eq. (2) to Eq. (4), the transfer efficiency can be rewritten as:

$$\eta = \left|\frac{2\mathrm{j}\omega M\sqrt{R_S R_L}}{(\omega M)^2 + \left(R_S + R_t + \mathrm{j}\omega L_t - \mathrm{j}\omega C_t\right)\left(R_L + R_r + \mathrm{j}\omega L_r - \mathrm{j}\omega C_r\right)}\right|^2 \tag{6}$$

When the resonant loops are designed to oscillate at the same frequency, the power transfer between loops is maximal, and the system works at maximum transfer efficiency. The tuned external capacitors connected to the transmitting and receiving loops can be calculated by:

$$C_i = \frac{1}{4\pi^2 f^2 L_i} \tag{7}$$

where $C_i(i=t,r)$ is the required capacitance to resonate the transmitting and receiving loops, f the frequency of source, and $L_i(i=t,r)$ the inductance of the resonant loops.

In the MRC-WPT system, the resistance of the resonant loops can be ignored compared with the resistance of the source and the load due to the small number of turns. At the resonant frequency, Eq. (5) is simplified as:

$$\eta = \left| \frac{2\mathrm{j}\omega M\sqrt{R_S R_L}}{(\omega M)^2 + R_S R_L} \right|^2 \tag{8}$$

For a fixed MRC-WPT system, it can be observed from Eq. (7) that the power transfer ability is mainly dependent on the mutual inductance between resonant loops.

In the MRC-WPT system, spiral coils are usually applied as the resonant loops. According to the magnetic field theory, the mutual inductance between the coils can be computed as:

$$\begin{cases} M = \sum_{i=1}^{n_t}\sum_{j=1}^{n_r} M_{ij}(r_i, r_j, d) \\ r_i = r_{out\_t} - (i-1)(w_t + s_t) - \dfrac{w_t}{2} \\ r_j = r_{out\_r} - (j-1)(w_r + s_r) - \dfrac{w_r}{2} \\ M_{ij}(r_i, r_j, d) = \dfrac{2\mu_0}{k}\sqrt{r_i r_j}\left[\left(1 - \dfrac{k^2}{2}\right)K(k) - E(k)\right] \\ k(r_i, r_j, d) = \sqrt{\dfrac{4r_i r_j}{(r_i + r_j)^2 + d^2}} \\ K(k) = \displaystyle\int_0^{\frac{\pi}{2}} \frac{1}{\sqrt{1 - k^2\sin^2\beta}}\mathrm{d}\beta \\ E(k) = \displaystyle\int_0^{\frac{\pi}{2}} \sqrt{1 - k^2\sin^2\beta}\mathrm{d}\beta \end{cases} \tag{9}$$

where M is the mutual inductance between coils of multiple turns; n_t and n_r are the numbers of turns for the transmitting coil and receiving coil; r_i and r_j are the equivalent radius of every turn; r_{out_t} and r_{out_r} are the outer radius of the loops; w_t and w_r are the wire diameters; s_t and s_r are the distance between turns; M_{ij} is the mutual inductance between coils of single turn; μ_0 is the permeability of free space; d is the distance between loops; $K(k)$ and $E(k)$ are respectively the complete elliptic integrals of the first and second kind.

Spiral coils with the same configuration are usually used in the conventional MRC-WPT system. Based on Eq. (8), it can be deduced that k tends to approach 1 when the distance between loops d decreases for identical resonant loops, which causes M increase dramatically. This is called magnetic over-coupling, and frequency splitting is observed from the transfer efficiency with two distinct peaks when the resonant loops get close to each other. In this case, the transfer efficiency peaks are no longer at the resonant frequency. Consequently, the performance of the MRC-WPT system operating at the fixed resonant frequency is deteriorated as the transfer efficiency drops, and the transfer power decreases.

The main objective of this work is to improve the performance of the MRC-WPT system by proposing an optimized loop based on the optimization of a conventional loop. Herein, a novel configuration of resonant loops is introduced to stabilize the magnetic coupling, as depicted in Fig. 3. The novel resonant loops are constructed with the same wire length ($l_t = l_r$). Besides, the wire diameter and coil outer radius are identical ($w_t = w_r$, $r_{out\_t} = r_{out\_r}$). However, the distances between turns of the coils are different ($s_t \neq s_r$). From Eq. (8), it can be deduced that the distance between turns will affect the mutual inductance between resonant loops.

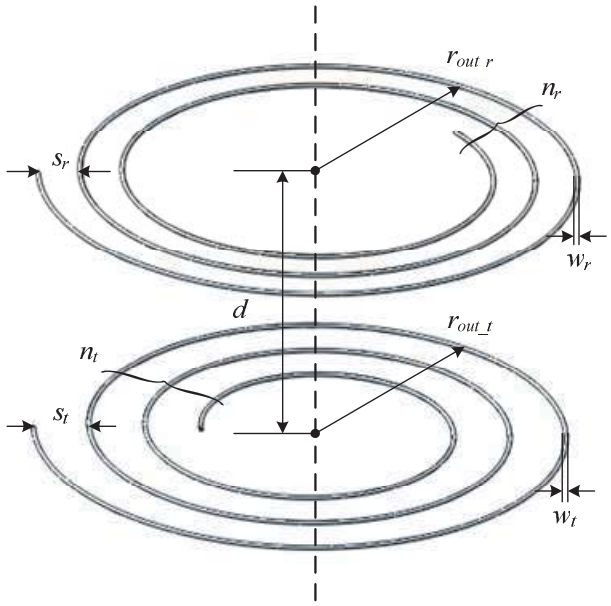

Figure 3. Configuration of the proposed resonant loops.

3. NUMERICAL INVESTIGATION

The transfer efficiency of the MRC-WPT system is strongly dependent on the geometrical parameters of the resonant loops. In this section, the performance of the MRC-WPT system with the proposed resonant loops will be compared with the performance of the conventional MRC-WPT system. Resonant loops with different distance between turns will be investigated, and an optimal configuration can be obtained. In addition, the sensitivity of the MRC-WPT system to misalignments with the optimal resonant loops will be studied.

The transmitting and receiving coils are connected to the source and the load, respectively. External capacitors are required by the coils to form resonant tank. In the calculation, the resonant frequency is set to 5 MHz, and the geometrical parameters of the resonant loops are listed as follows: the outer radii of the transmitting and receiving coils, r_{out_t} and r_{out_r}, are 100 mm; the wire diameters, w_t and w_r, are 1.4 mm; the number of turns of the transmitting coil, n_t, is 6. The MRC-WPT system with such size of coils is suitable for the powering of some electronic products. The total wire lengths of the transmitting and receiving coils are both equal to 2.073 m. For a fixed wire length, the distance between turns of the receiving coil is tuned to vary from $s_r = 1$ mm to $s_r = 15$ mm with a step of 2 mm. Consequently, the number of turns for the receiving coil also changes. When calculating the mutual inductance in Eq. (8), the number of turns for the resonant coils is supposed to be positive integers. However, the number of turns for the receiving coil may not be an integer when the distance between turns varies in this study. Therefore, mathematical calculation of the mutual inductance may cause error. In this study, all the numerical analysis is performed by ANSOFT Maxwell which is developed based on finite element method and suitable to solve the electromagnetic problem.

In the study, the distance between turns of the transmitting coil, s_t, is equal to 15 mm, and the distance between turns of the receiving coil s_r changes from 1 mm to 15 mm with the step of 2 mm. The resonant loops when $s_t = s_r = 15$ mm are regarded as the conventional loops while the resonant loops when s_t is not equal to s_r are considered as the proposed resonant loops. It can be found that the mutual inductance is sensitive to the variation of s_r, which tends to be more uniform with the decrease of distance between turns. The mutual inductance at shorter distance gets smaller while the mutual inductance at longer distance becomes larger than the conventional loops. For clear observation, Fig. 4 only shows how the mutual inductance and transfer efficiency vary with the distance when using the proposed resonant loops ($s_t = 15$ mm, $s_r = 1$ mm, $s_r = 5$ mm, and $s_r = 15$ mm) and the conventional

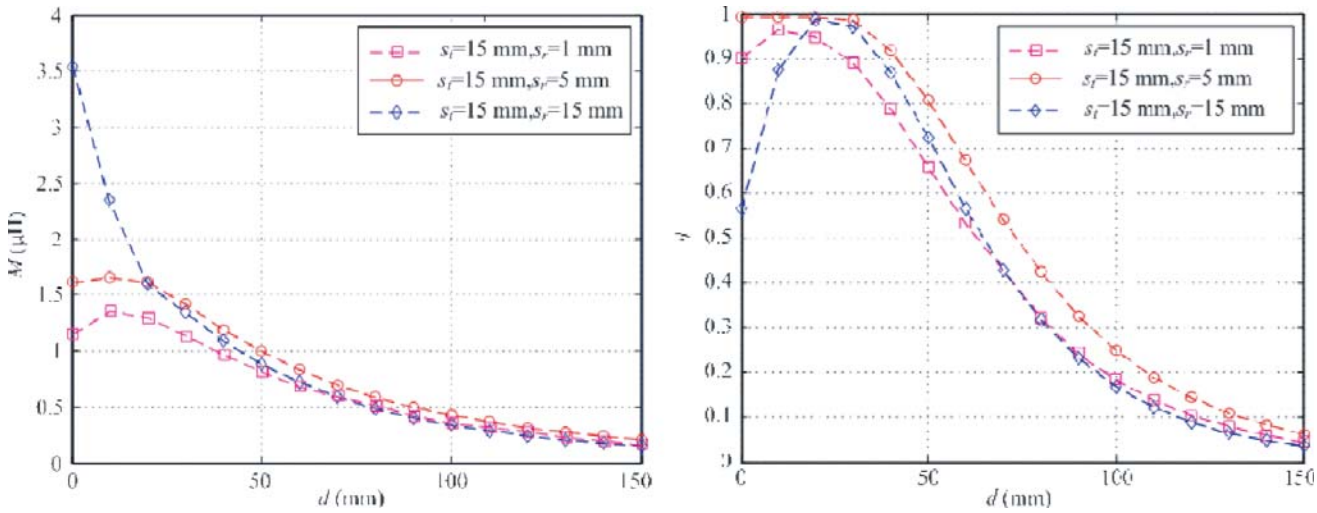

(a) (b)

Figure 4. Mutual inductance and transfer efficiency versus transfer distance with distance between turns variation. (a) Mutual inductance versus transfer distance. (b) Transfer efficiency versus transfer distance.

loops ($s_t = s_r = 15\,\text{mm}$). The rapid increase of mutual inductance at short distance results in the decrease of transfer efficiency for the conventional loops due to frequency splitting. However, by changing the distance between turns which means that the number of turns also varies, the mutual inductance of the proposed resonant loops can be tuned to change in a more uniform variation than the conventional identical resonant loops. The magnetic coupling strength can be lessened when the receiving coil moves close to the transmitting coil. Furthermore, the mutual inductance can be strengthened for a longer distance. As a result, the performance of the MRC-WPT system is improved.

Figure 5 shows the average transfer efficiency when the distance between turns changes for three different ranges of transfer distance. It can be observed that the average transfer efficiency increases first and then decreases when s_r changes from 1 mm to 15 mm. When s_r is 5 mm, the average transfer efficiency is the highest among the proposed resonant loops, which is about 10% higher than the conventional loops. It can also be seen from Fig. 4 that the performance of the MRC-WPT system when s_r is 5 mm outperforms the conventional system. Based on the above analysis, the optimal geometrical parameters of the proposed resonant loops are shown in Table 1.

Table 1. Parameters of the proposed optimal resonant loops.

Dimension	Transmitter	Receiver
Outer radius	100 mm	100 mm
Wire length	2.073 m	2.073 m
Wire diameter	1.4 mm	1.4 mm
Number of turns	6	3.6
Distance between turns	15 mm	5 mm

Figure 6 compares the transfer efficiency versus frequency when the transfer distance varies for the conventional and the proposed optimal resonant loops. It can be drawn from Fig. 6(a) that frequency splitting occurs when the transfer distance decreases from 20 mm to 0 mm for the conventional resonant loops while it can be avoided with the proposed loops as shown in Fig. 6(b). Additionally, the transfer efficiency of the MRC-WPT system with the proposed resonant coils keeps higher than the conventional one at the resonant frequency, indicating more excellent power transfer ability.

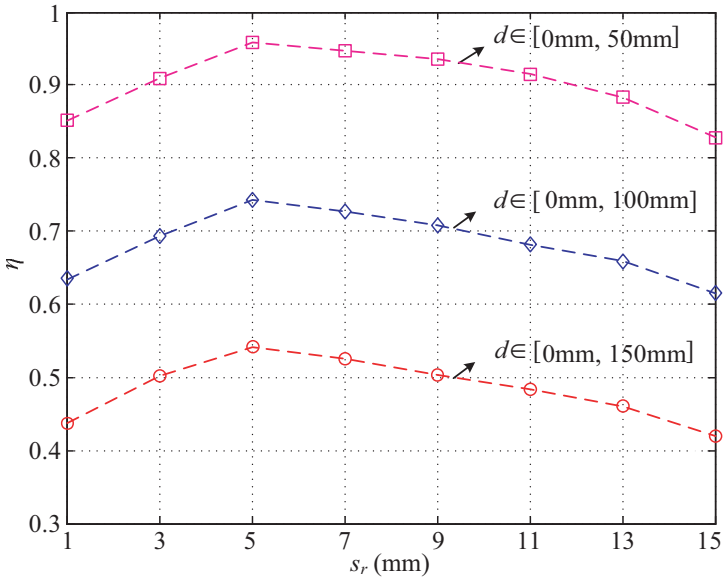

Figure 5. Average transfer efficiency for three different range of transfer distance.

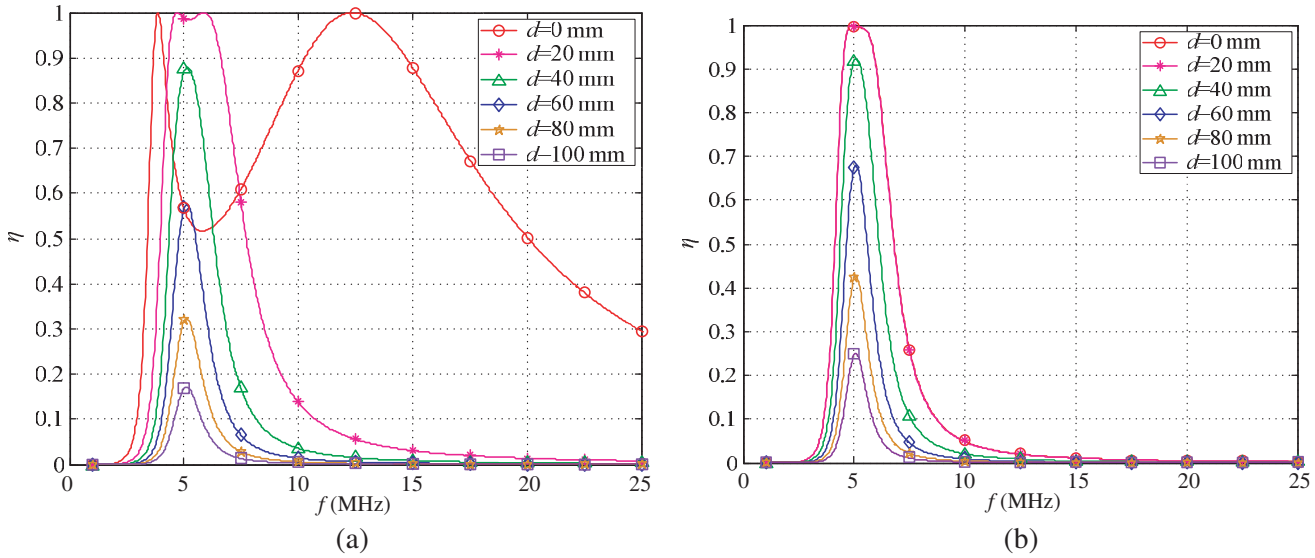

Figure 6. Transfer efficiency versus frequency when transfer distance varies (a) for conventional resonant loops, (b) for the proposed optimal resonant loops.

The performance of the proposed system in the case of lateral or angular misalignment is also investigated. Fig. 7 presents the lateral misalignment between the resonant loops. The receiving coil is moving in a parallel orientation with lateral displacement x at a fixed transfer distance d.

For lateral misalignments at different transfer distances, the variation of mutual inductance and transfer efficiency for the proposed optimal resonant loops is presented and compared with the conventional loops in Fig. 8. Lateral misalignment is commissioned from $x = -100$ mm to $x = 100$ mm with a step of 10 mm. The distance between the transmitting coil and receiving coil is also altered from $d = 20$ mm to $d = 100$ mm with a step of 20 mm. It can be observed from Fig. 8 that the mutual inductance and transfer efficiency decline with the increase of the transfer distance. Besides, a larger lateral misalignment leads to deterioration of the mutual inductance and transfer efficiency.

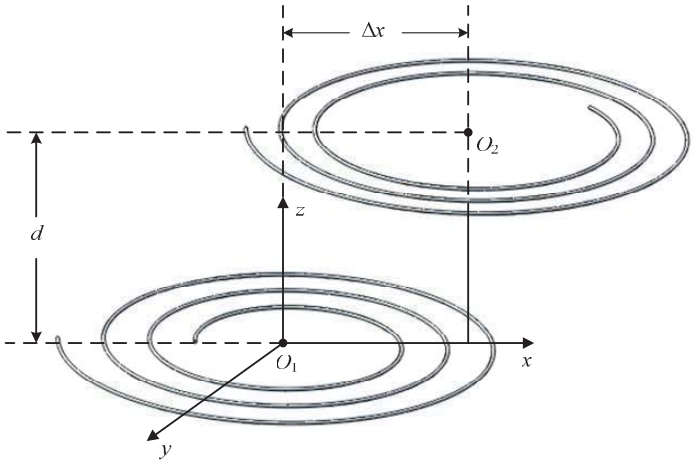

Figure 7. Lateral misalignment between resonant loops.

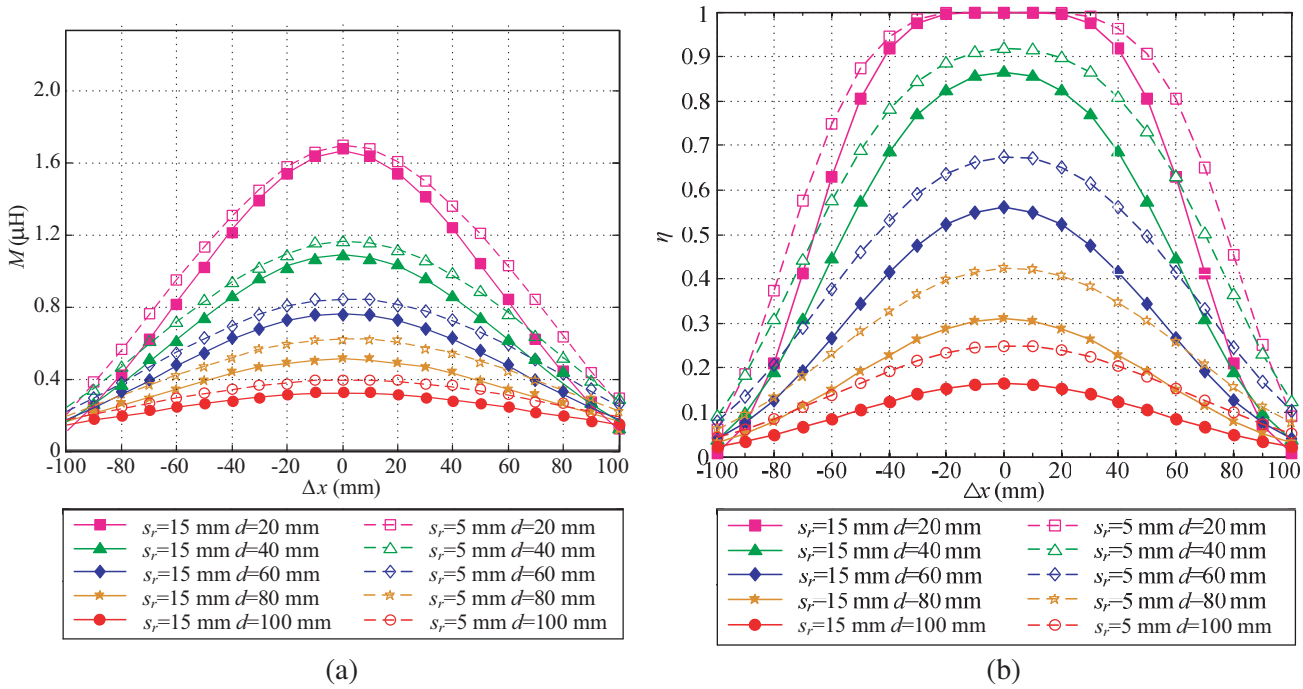

Figure 8. Mutual inductance and transfer efficiency against lateral misalignments. (a) Mutual inductance against lateral misalignments. (b) Transfer efficiency against lateral misalignments.

At a fixed transfer distance, the mutual inductance of the proposed resonant loops is higher than that of the conventional loops when the lateral misalignment varies, as shown in Fig. 8(a). Accordingly, the transfer efficiency shows an obvious increase for the MRC-WPT system with the proposed loops compared to the conventional one as depicted in Fig. 8(b). It should be noted that the performance of the proposed system is also sensitive to x just as the conventional MRC-WPT system.

In addition to the lateral misalignment, angular misalignment is also a crucial factor that affects the system efficiency. Fig. 9 shows the angular misalignment between the resonant loops. The receiving coil is moving to form an angular misalignment α against the central axis at a fixed transfer distance d.

For angular misalignments at different transfer distances, the variation of mutual inductance and transfer efficiency for the proposed optimal and conventional resonant loops is illustrated in Fig. 10.

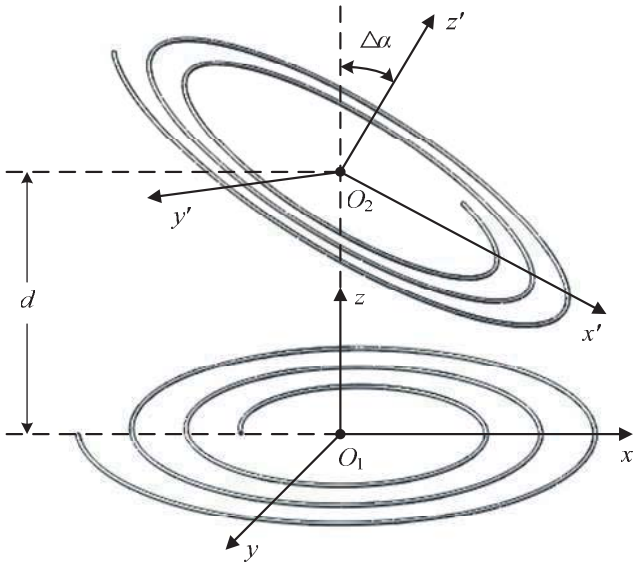

Figure 9. Angular misalignment between resonant loops.

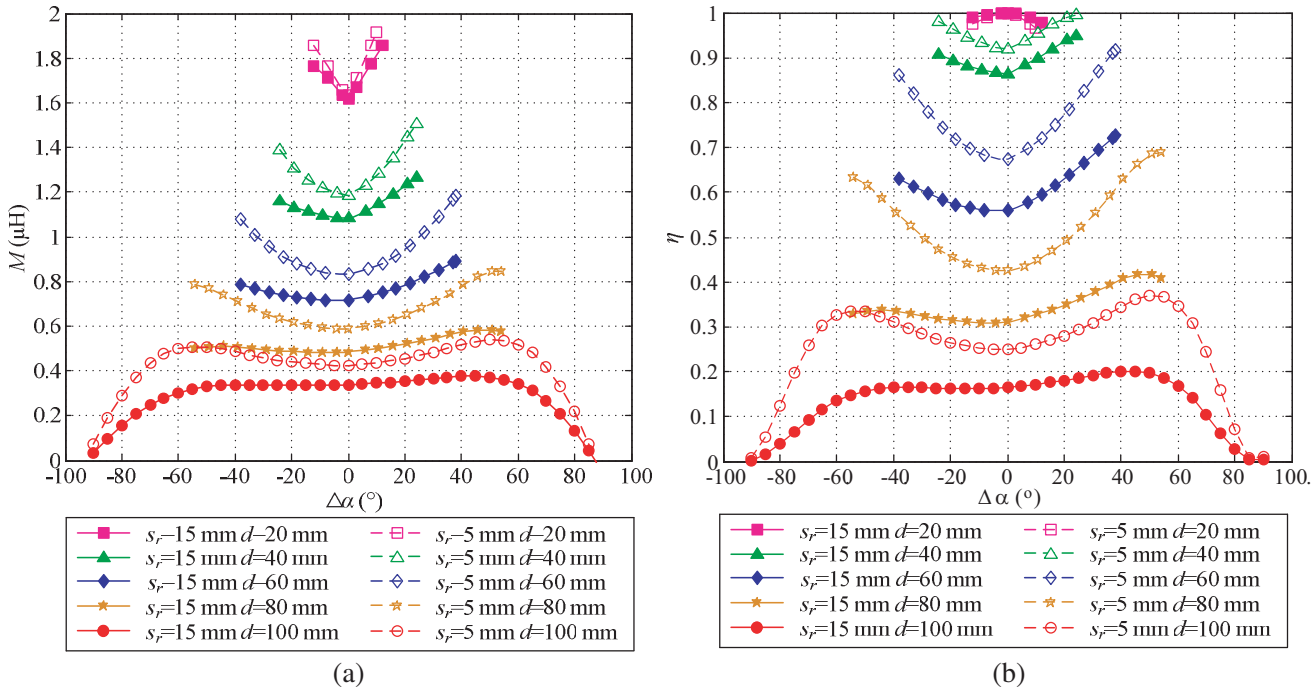

Figure 10. Mutual inductance and transfer efficiency against angular misalignments. (a) Mutual inductance against angular misalignments. (b) Transfer efficiency against angular misalignments.

Considering the loops geometry, different ranges of angular misalignments with a step of 5° are conducted at transfer distances varying from $d = 20$ mm to $d = 100$ mm with a step of 20 mm. It can be seen from Fig. 10(a) that the mutual inductance at shorter distance is much higher than that at longer distance for both loops. The transfer efficiency shows a similar changing trend as shown in Fig. 10(b). In the case of angular misalignments, the mutual inductance and transfer efficiency of the MRC-WPT system with the proposed novel resonant loops have better performance than that with conventional loops. For

$d = 20\,\text{mm}$, the transfer efficiency is a bit smaller for the proposed loops and nearly coincides with the conventional loops due to the approximation of the mutual inductance. Besides, the system efficiency declines with angular misalignments caused by magnetic over-coupling as the mutual inductance is higher than that when $\alpha = 0°$. With $d = 40\,\text{mm}$, $60\,\text{mm}$, and $80\,\text{mm}$, when angular misalignments occur, the system efficiency and mutual inductance are larger than that when $\alpha = 0°$. For $d = 100\,\text{mm}$, the mutual inductance increases first, then decreases with the angular misalignment. The variation of the transfer efficiency is consistent with the mutual inductance. Similar to the conventional system, the performance of the proposed system is also affected by the angular misalignment.

4. EXPERIMENTAL IMPLEMENTATION AND VALIDATION

To validate the simulation results, a practical MRC-WPT system equipped with the proposed optimal resonant loops (T_1, R_1) is fabricated based on the geometrical parameter presented in Table 1, as shown in Fig. 11. For comparison, the conventional resonant loops are also implemented in which the receiving coil (R_2) is identical with the transmitting coil (T_2). The operating frequency of the MRC-WPT system is 5 MHz. The measured electrical parameters of the coils are: $L_{T1} = 4.1\,\mu\text{H}$, $L_{R1} = 5.3\,\mu\text{H}$, $L_{T2} = L_{R2} = 4.1\,\mu\text{H}$, $R_{T1} = R_{R1} = R_{T2} = R_{R2} = 0.05\,\Omega$. The compensated capacitance of coils T_1, R_1, T_2, and R_2 can be calculated by Eq. (6): $C_{T1} = 254\,\text{pF}$, $C_{R1} = 191\,\text{pF}$, $C_{T2} = C_{R2} = 254\,\text{pF}$. In the experiment, the transmitting coil is positioned in parallel with the receiving coil on the same axis separated by distance d.

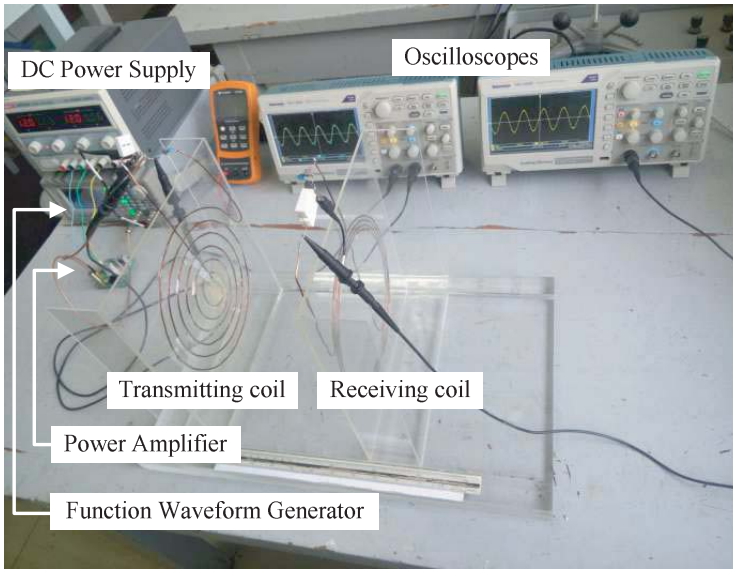

Figure 11. Experimental setup of the MRC-WPT system with the proposed resonant loops.

Figure 12 shows the variation of mutual inductance between resonant loops for the proposed and conventional geometries. When the distance between the transmitting coil and receiving coil changes from 150 mm to 0 mm, the mutual inductance of the conventional loops increases from 0.12 µH to 2.96 µH. As for the proposed loops, the mutual inductance alters from 0.19 µH to 1.51 µH, which indicates a smaller and more uniform variation. In addition, larger mutual inductance at longer distance enhances power transfer ability, and smaller mutual inductance at shorter distance suppresses magnetic over-coupling. Compared with the simulated mutual inductance, the measured results are a bit smaller. This is mainly because the distance in the experiment cannot be controlled exactly the same as that in the simulation.

The variation of the mutual inductance is directly related to the performance of an MRC-WPT system. Fig. 13 compares the measured output voltage obtained with the proposed and conventional MRC-WPT systems. When the distance changes between 0 mm and 150 mm, the measured voltage

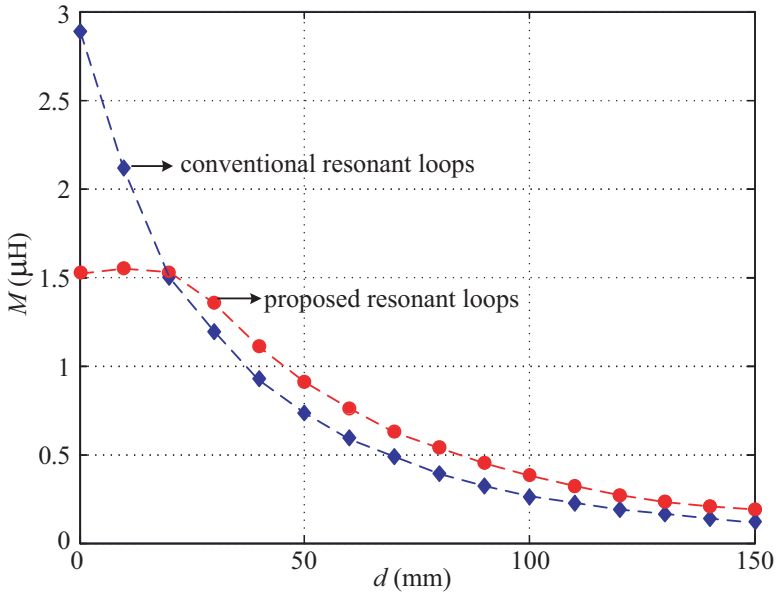

Figure 12. Measured mutual inductance of the proposed and conventional resonant loops.

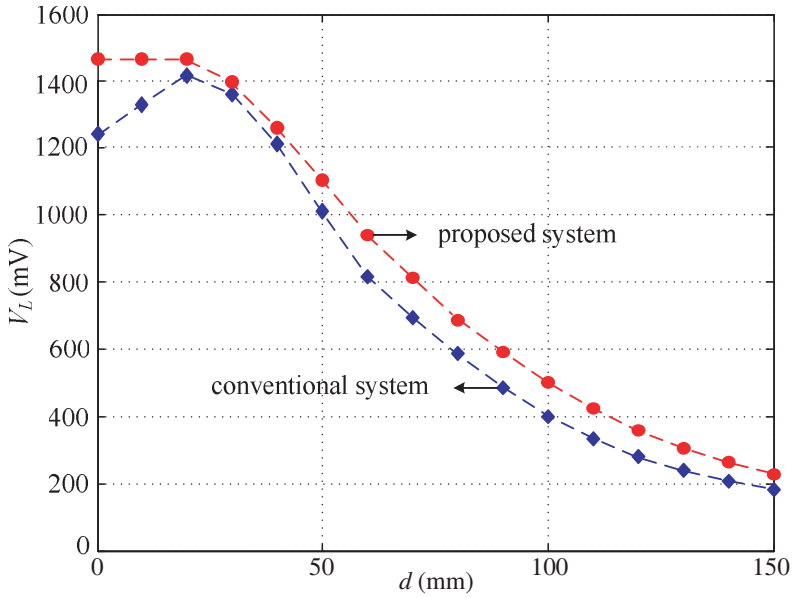

Figure 13. Measured output voltage of the proposed and conventional MRC-WPT system.

of the proposed scheme keeps higher than that of the conventional scheme for the whole range. The output voltage of the conventional MRC-WPT system decreases due to frequency splitting when the distance alters from 20 mm to 0 mm. In contrast, the proposed MRC-WPT system maintains a relatively constant output voltage at short distance. For longer distance, the output voltage of the proposed scheme is improved. It can be predicted that smaller variation of mutual inductance ensures a better performance of the system.

Both simulated and experimental results have validated the excellent performance of the proposed resonant loops in the power transfer. The main reason that the proposed loops are superior to the conventional one is explained as follows. From Eq. (8), it can be found that k approaches 1 if the receiving coil moves close to the transmitting coil for loops with the same radius. Correspondingly, $K(k)=\infty$

and $E(k)$=1. This makes the rapid increase of mutual inductance and over-coupling of magnetic field occurs. In this work, the distance between turns for the receiving coil is different from that for the transmitting coil. In other words, the equivalent radius of the coils is different which restrains k from 1, and frequency splitting caused by magnetic field over-coupling is inhibited.

To validate the performance of the proposed MRC-WPT system in case of misalignments, lateral and angular misalignments between resonant loops are carried out in the experiment at the transfer distance $d = 60$ mm.

Figure 14 presents the output voltage on the load for the proposed and conventional MRC-WPT

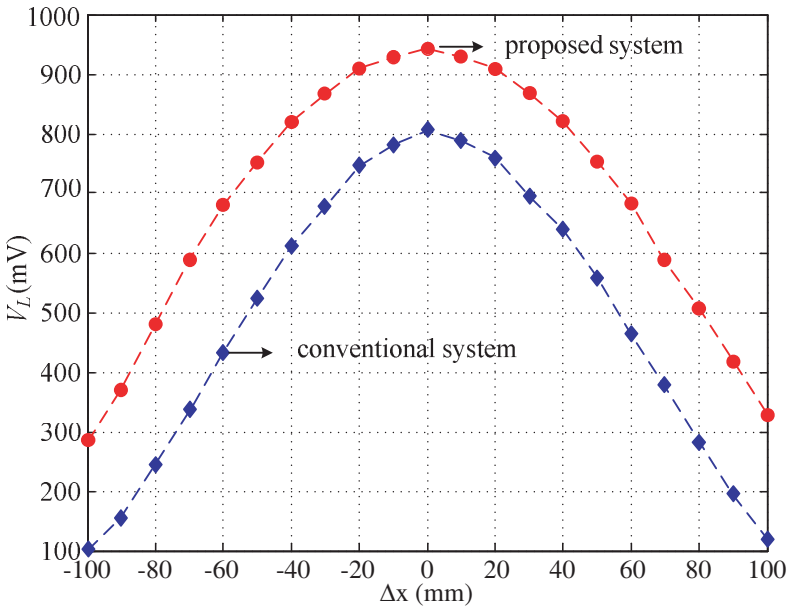

Figure 14. Measured output voltage of the proposed and conventional MRC-WPT system in case of lateral misalignment.

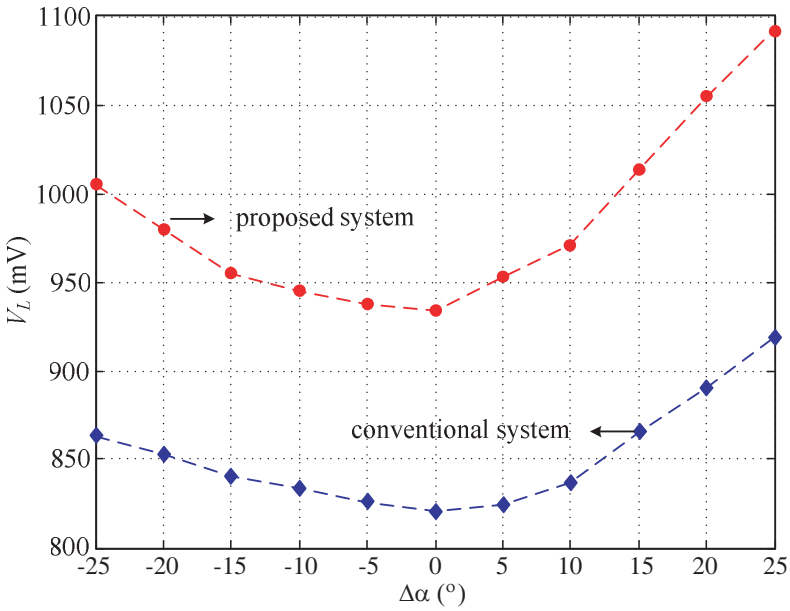

Figure 15. Measured output voltage of the proposed and conventional MRC-WPT system in case of angular misalignment.

systems in case of lateral displacement. It can be observed that the proposed system outperforms the conventional one. On average, the output voltage of the proposed system is about 190 mV higher than the conventional system when the lateral misalignment alters between −100 mm and 100 mm.

Figure 15 plots the output voltage on the load for the proposed and conventional MRC-WPT systems in case of angular misalignment. It can be obtained that the output voltage of the proposed system is in average 135 mV higher than that of conventional one when the angular misalignment is between -25° and 25°. At the symmetric position of $\alpha = 0^\circ$, the output voltage of the positive angular misalignment is higher than that of the negative misalignment. This is because related magnetic coupling is stronger as shown in Fig. 10(a).

5. CONCLUSION

In this paper, an MRC-WPT system with novel resonant loops has been proposed. Based on the theoretical models and numerical analysis, the proposed resonant loops are optimized to suppress magnetic over-coupling and eliminate frequency splitting when the receiving coil comes close to the transmitting coil. Additionally, the magnetic coupling is also strengthened for longer distance between loops. Compared with the conventional MRC-WPT system, the proposed system is less sensitive to transfer distance, and the average transfer efficiency is improved by 10% without adding any complicated control circuits. In the cases of lateral and angular misalignments, the proposed MRC-WPT system shows better performance than the conventional scheme. Experimental results have validated the performance of the proposed MRC-WPT system. It should be mentioned that the idea proposed in this work can also be applied in the practical wireless power transfer system with other sizes of coils.

ACKNOWLEDGMENT

This work was supported by the National Natural Science Foundation of China under Grants U1904182 and U1704134, and the Foundation for University Key Young Teacher by Henan Province of China under Grant Nos. 2017GGJS040 and 2020GGJS061.

REFERENCES

1. Wang, Q. H., W. Q. Che, M. Dionigi, and F. Mastri, "Gains maximization via impedance matching networks for wireless power transfer," *Progress In Electromagnetics Research*, Vol. 164, 135–153, 2019.
2. Kalwar, K. A., M. Aamir, and S. Mekhilef, "A design method for developing a high misalignment tolerant wireless charging system for electric vehicles," *Meas.*, Vol. 118, 237–245, 2018.
3. Sahany, S., S. Biawal, D. P. Kar, P. K. Sahoo, and S. Bhuyan, "Impact of functioning parameters on the wireless power transfer system used for electric vehicle charging," *Progress In Electromagnetics Research M*, Vol. 79, 187–197, 2019.
4. Basar, M. R., M. Y. Ahmad, J. Cho, and F. Ibrahim, "An improved resonant wireless power transfer system with optimum coil configuration for capsule endoscopy," *Sensors and Actuators A Phys.*, Vol. 249, 207–216, 2017.
5. Liu, H., Q. Shao, and X. L. Fang, "Modeling and optimization of class-E amplifier at subnominal condition in a wireless power transfer system for biomedical implants," *IEEE Trans. Biomed. Circuits Syst.*, Vol. 11, No. 1, 35–43, 2017.
6. Jia, Y. Y., S. A. Mirbozorgi, P. C. Zhang, O. T. Inan, W. Li, and M. Ghovanloo, "A dual-band wireless power transmission system for evaluating mm-sized implants," *IEEE Trans. Biomed. Circuits Syst.*, Vol. 13, 307–595, 2017.
7. Portol, R. W., V. J. Brusamarello, I. Muller, F. L. C. Riano, and F. R. de Sousa, "Wireless power transfer for contactless instrumentation and measurement," *IEEE Instrum. Meas. Mag.*, Vol. 20, No. 4, 49–54, 2017.

8. Ho, S. L., J. Wang, W. N. Fu, and M. Sun, "A comparative study between novel witricity and traditional inductive magnetic coupling in wireless charging," *IEEE Trans. Magn.*, Vol. 47, No. 5, 1522–1525, 2011.
9. Shi, Y. Y., J. Liang, M. Wang, and Z. Zhang, "Efficient magnetic resonant coupling wireless power transfer with a novel conical-helix resonator," *IEICE Electron. Express.*, Vol. 14, No. 13, 1–6, 2017.
10. Samanta, S. and A. K. Rathore, "A new current-fed CLC transmitter and LC receiver topology for inductive wireless power transfer application: Analysis, design, and experimental results," *IEEE Trans. Transport. Electrific.*, Vol. 1, No. 4, 357–368, 2015.
11. Kallel, B., O. Kanoun, and H. Trabelsi, "Large air gap misalignment tolerable multi-coil inductive power transfer for wireless sensors," *IET Power Electron.*, Vol. 9, No. 8, 1768–1774, 2016.
12. Jeong, N. S. and C. F. arobolante, "Wireless charging of a metal-body device," *IEEE Trans. Microw. Theory Tech.*, Vol. 65, No. 4, 1077–1086, 2017.
13. Kurs, A., et al., "Wireless power transfer via strongly coupled magnetic resonances," *Science*, Vol. 317, No. 5834, 83–86, 2007.
14. Shi, Y. Y., Y. M. Zhang, M. H. Shen, Y. Fan, C. Wang, and M. Wang, "Design of a novel receiving structure for wireless power transfer with the enhancement of magnetic coupling," *AEU — Int. J. Electron. Commun.*, Vol. 95, 236–241, 2018.
15. Wang, M., J. Feng, Y. Y. Shi, and M. H. Shen, "Demagnetization weakening and magnetic field concentration with ferrite core characterization for efficient wireless power transfer," *IEEE Trans. Ind. Electron.*, Vol. 66, No. 3, 1842–1851, 2019.
16. Ye, Z. H., Y. Sun, X. Dai, C. S. Tang, Z. H. Wang, and Y. G. Su, "Energy efficiency analysis of U-coil wireless power transfer system," *IEEE Trans. Power Electron.*, Vol. 31, No. 7, 4809–4817, 2016.
17. Narayanamoorthi, R., A. Vimala Juliet, and B. Chokkalingam, "Frequency splitting-based wireless power transfer and simultaneous propulsion generation to multiple micro-robots," *IEEE Sensors J.*, Vol. 18, No. 13, 5566–5575, 2018.
18. Zhang, X. Y., C. D. Xue, and J. K. Lin, "Distance-insensitive wireless power transfer using mixed electric and magnetic coupling for frequency splitting suppression," *IEEE Trans. Microw. Theory Techn.*, Vol. 65, No. 11, 4307–4316, 2017.
19. Wang, M., C. Zhou, Y. Y. Shi, M. H. Shen, and J. Feng, "Development of a novel spindle-shaped coil-based wireless power transfer system for frequency splitting elimination," *Int. J. of Circuit Theory Appl.*, Vol. 48, No. 3, 356–368, 2020.
20. Huang, S. D., Z. Q. Li, and K. Y. Lu, "Frequency splitting suppression method for four-coil wireless power transfer system," *IET Power Electron.*, Vol. 9, No. 15, 2859–2864, 2016.
21. Liu, Z., Z. Z. Chen, J. Y. Li, Y. L. Guo, and B. Xu, "A planar L-shape transmitter for a wireless power transfer system," *IEEE Antennas Wireless Propag. Lett.*, Vol. 16, 960–963, 2017.
22. Tang, X., J. X. Zeng, K. P. Pun, S. P. Mai, and C. Zhang, "Low-cost maximum efficiency tracking method for wireless power transfer systems," *IEEE Trans. Power Electron.*, Vol. 33, No. 6, 5317–5329, 2018.
23. Yeo, T. D., D. S. Kwon, S. T. Khang, and J. W. Yu, "Design of maximum efficiency tracking control scheme for closed-loop wireless power charging system employing series resonant tank," *IEEE Trans. Power Electron.*, Vol. 32, No. 1, 471–478, 2017.
24. Kim, J., D. H. Kim, and Y. J. Park, "Free-positioning wireless power transfer to multiple devices using a planar transmitting coil and switchable impedance matching networks," *IEEE Trans. Microw. Theory Techn.*, Vol. 64, No. 11, 3714–3722, 2016.
25. Huang, Y., N. Shinohara, and T. Mitani, "Impedance matching in wireless power transfer," *IEEE Trans. Microw. Theory Techn.*, Vol. 65, No. 2, 582–590, 2017.
26. Lee, W. S., W. I. Son, K. S. Oh, and J. W. Yu, "Contactless energy transfer systems using antiparallel resonant loops," *IEEE Trans. Ind. Electron.*, Vol. 60, No. 1, 350–359, 2013.
27. Kim, J. and J. Jeong, "Range-adaptive wireless power transfer using multiloop and tunable matching techniques," *IEEE Trans. Ind. Electron.*, Vol. 62, No. 10, 6233–6241, 2015.

28. Lee, G., B. H. Waters, Y. G. Shin, J. R. Smith, and W. S. Park, "A reconfigurable resonant coil for range adaptation wireless power transfer," *IEEE Trans. Microw. Theory Techn.*, Vol. 64, No. 2, 624–632, 2016.
29. Lee, W. S., W. I. Son, K. S. Oh, and J. W. Yu, "Contactless energy transfer systems using antiparallel resonant loops," *IEEE Trans. Ind. Electron.*, Vol. 60, No. 1, 350–359, 2013.
30. Lyu, Y. L., F. Y. Meng, G. H. Yang, B. J. Che, Q. Wu, L. Sun, et al., "A method of using nonidentical resonant coils for frequency splitting elimination in wireless power transfer," *IEEE Trans. Power Electron.*, Vol. 30, No. 11, 6097–6107, 2015.
31. Zhang, Y. M., Z. M. Zhao, and K. N. Chen, "Frequency-splitting analysis of four-coil resonant wireless power transfer," *IEEE Trans. Ind. Appl.*, Vol. 50, No. 4, 2436–2445, 2014.
32. Song, K., G. Yang, Y. Guo, Y. Lan, S. Dong, J. H. Jiang, and C. B. Zhu, "Design of DD coil with high misalignment tolerance and low EMF emissions for wireless electric vehicle charging systems," *IEEE Trans. Power Electron.*, Vol. 35, No. 9, 9034–9045, 2020.
33. Yu, T. C., W. H. Huang, and C. L. Yang, "Design of dual frequency mixed coupling coils of wireless power and data transfer to enhance lateral and angular misalignment tolerance," *IEEE J. Electromagn. RF Microw. M. Biol.*, Vol. 3, No. 3, 216–223, 2019.
34. Lee, W. S., S. Park, J. H. Lee, and M. M. Tentzeris, "Longitudinally misalignment-insensitive dual-band wireless power and data transfer systems for a position detection of fast-moving vehicles," *IEEE Trans. Antennas Propag.*, Vol. 67, No. 8, 5614–5622, 2019.
35. Hu, H. and S. V. Georgakopoulos, "Multiband and broadband wireless power transfer systems using the conformal strongly coupled magnetic resonance method," *IEEE Trans. Ind. Electron.*, Vol. 64, No. 5, 3595–3607, 2017.
36. Jiang, C. C., C. D. Hu, Y. H. Xie, S. Y. Chen, Q. L. Cui, and Y. L. Xie, "Analysis and experimental study of impedance matching characteristic of RF ion source on neutral beam injector," *IEEE Plasma Sci.*, Vol. 46, No. 7, 2677–2679, 2018.